CHEMISTRY
A EUROPEAN JOURNAL

DOI: 10.1002/chem.200701220

Assessable Consequences of Through-Bond Donor–Acceptor Interactions in β-Aminoketones

Andrew J. Lampkins, Yan Li, Alexandre Al Abbas, Khalil A. Abboud, Ion Ghiviriga, and Ronald K. Castellano*[a]

In memory of Professor Dmitry M. Rudkevich

Abstract: Reported are the syntheses of ester-functionalized (**6**–**8**) and alkyl-substituted (**9**) 1-aza-adamantanones; the easy handling of the compounds provides an opportunity to comprehensively study the fundamental changes in structure and reactivity that can accompany the donor–acceptor arrangement in rigid β-aminoketones. X-ray structural analysis of trione **6** and dione **7** reveals bond length and angle variations consistent with through-bond (hyperconjugative) donor–acceptor interactions. Observed is a shortening of the C–N bond, elongation of the central C–C bond (to ≈1.6 Å), and a significant pyramidalization of the carbonyl carbon within the donor–σ-acceptor pathway. UV/Vis spectra of **6**–**9** show a new absorption maximum (λ_{max} = 260–275 nm in three solvents), the so-called "σ-coupled transition"; the molar absorptivity scales with the number of carbonyl groups (for trione **6**, $\varepsilon \approx 3000$, for dione **7**, $\varepsilon \approx 2000$) and the band reversibly disappears upon addition of acid. IR and ^{13}C NMR spectroscopic data show trends consistent with through-bond donation to the carbonyl acceptor groups and commensurate weakening of the carbonyl π bond. High yielding acid-mediated fragmentations are used to illustrate the effects of the donor–acceptor arrangement on the reactivity of the molecules. Given that donor–σ-acceptor molecules have recently been found to show self-assembly behavior and macromolecular properties linked to their unusual structure, the current analysis encourages further consideration of the systems in advanced materials applications.

Keywords: donor–acceptor systems · hyperconjugation · reactivity · strained molecules · through-bond interactions

Introduction

Cyclic β-aminoketone derivatives are unique molecular models to determine the effects of through-bond[1] (hyperconjugative[2]) interactions on structure, reactivity, stereoselectivity, and photophysical properties. The donor (amine) and acceptor (carbonyl) interaction is optimized when the nitrogen lone pair, C_α–C_β bond, and carbonyl π system (Figure 1) are in a zig–zag arrangement; this situation is transiently maintained for molecules such as *N*-methylpiperidone **1** and tropinone **2**, but permanently fixed in aza-adamantanones **3** (and related structures; Figure 1). Arrival at the desired donor–acceptor geometry (with respect to the saturated two-carbon bridge) in the donor–σ-acceptor molecules[3] is often associated with a unique (split) π–π* absorption (σ-coupled transition:[4] λ_{max} = 220–260 nm; ε = 500–

[a] A. J. Lampkins, Y. Li, A. Al Abbas, Dr. K. A. Abboud, Dr. I. Ghiviriga, Prof. R. K. Castellano
Department of Chemistry, University of Florida
P.O. Box 117200, Gainesville, FL 32611 (USA)
Fax: (+1) 352-846-0296
E-mail: castellano@chem.ufl.edu

Supporting information for this article is available on the WWW under http://www.chemeurj.org/ or from the author.

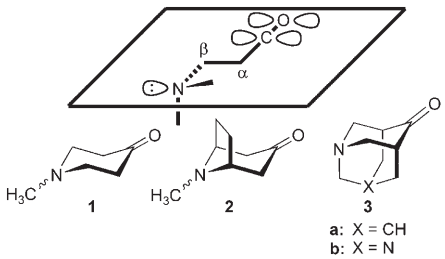

Figure 1. Donor–σ-acceptor arrangement in cyclic β-aminoketones; *N*-methylpiperidone (**1**), tropinone (**2**), 1-aza-adamantanone (**3a**), and 1,3-diaza-adamantanone (**3b**). Note that the appropriate nitrogen configuration is fixed only in **3a** and **3b**.

2500) and a red-shifted ($\lambda_{max}=285$–315 nm; $\varepsilon=30$–50) and intensified n–π* absorption in the UV spectra.[4,5] Studies that attribute ground-state structural and related reactivity changes to donor–σ-acceptor interactions in β-aminoketones have often done so despite the presence of competing (and often times stronger) inductive, electrostatic, steric, and/or solvation effects. Even so, the most carefully constructed examples show that donor–acceptor through-bond interactions can play at least a supporting role in perturbations of structure and reactivity in these systems.

Recently we have exploited the unusual 1-aza-adamantanetrione[6] (AAT) (Figure 2) framework to explore the consequences of donor–acceptor through-bond interactions at

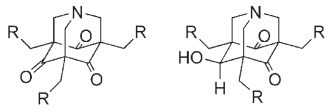

4: R = Ar
5: R = CONHAr
6: R = CO_2-*i*Pr
8: R = CH_2CO_2-*i*Pr
9: R = C_4H_9
7: R = CO_2-*i*Pr

Figure 2. 1-Aza-adamantanones considered in the previous and current studies.

the macromolecular/supramolecular level.[7] Molecules like **4**, for example, form gel phases at low concentration in organic solution, a consequence of their shape (conformational preferences), ground-state dipole (and dipolar interactions), and aromatic substituents.[7a] Installation of amide functional groups proximal to the AAT core causes remarkable changes in macromolecular behavior as shown by **5**; aggressive solution-phase assembly is observed that also results in the molecule's displaying long-range order in the solid state.[7b] The enhancement is not, based on IR and NMR studies, exclusively (or even mainly) the result of more conventional intermolecular hydrogen bonding between monomers, but rather well-defined interactions between the polar amide groups and polar AAT core (that include weak intramolecular hydrogen-bonding contacts) that modulate conformational preferences, molecular dipole, and inter-/intramolecular dipolar interactions. More recent high-level computational work suggests a dramatic role of these amides in tuning the fundamental electronic properties of the molecules making them potentially suitable for electronic and optoelectronic applications.[7c,d] Although multiple interactions are at work, experimental and theoretical studies support the notion that through-bond interactions a) can be "tuned" in these systems and b) offer a subtle way to address the macromolecular properties that emerge upon molecular self-assembly.

Reported here are the syntheses of ester-functionalized aza-adamantanones (**6**–**8**, Figure 2) the easy handling of which provides an opportunity to better study the fundamental changes in structure and reactivity that can accompany the donor–σ-acceptor arrangement in these 1-aza-adamantanones, and β-aminoketones in general. Included is discussion of the first X-ray crystal structure of an AAT (**6**) and second reported structure of an aza-adamantanedione (AAD; **7**) that offer compelling structural evidence for through-bond interactions, complemented by spectroscopic (NMR, IR, and UV) studies and comparisons to the literature and appropriate model compounds **8** and **9**. The consequences of through-bond interactions on reactivity are discussed in the context of nitrogen basicity/nucleophilicity and an acid-promoted core fragmentation. The conclusion from the studies is that the through-bond donor–acceptor interactions in the aza-adamantanones are both assessable and significant enough to play a role in their ground-state structure, reactivity, and self-assembly properties.

Results and Discussion

Synthesis: Several ester-functionalized aza-adamantanones have been prepared for these studies (Schemes 1 and 2). In each case, isopropyl esters have been selected due to their efficient preparation under Fischer esterification conditions, good solubility (in part by discouraging aggregation of the core), and stability (to Lewis and protic acids, and mild bases). The first, **6** (Scheme 1), like **5**, bears only one methylene spacer between the core and ester carbonyl. To prepare **6**, triacid **10** (made in three steps from commercially available 1,3,5-trimethoxybenzene[7b]) is esterified to give triisopropyl ester **11** which is then deprotected with BBr_3 to afford the phloroglucinol cyclization substrate **12**.[8] Ester-functionalized AAT **6** is then formed upon reaction of **12** with hexamethylenetetramine (HMTA), in the appropriate alcoholic solvent (*i*PrOH) in 66% yield. This particular cyclization works best at higher concentrations (≥ 0.1 M). As expected, triisopropyl ester **6** is markedly more soluble than the previously synthesized amide derivative **5**.

The reasonable solubility of triester **6** allowed us to explore carbonyl hydride reductions at low temperatures with the goal of isolating and characterizing the corresponding alcohols, and analyzing the structural consequences of through-bond donor–acceptor interactions within a structurally related aza-adamantanone family. Indeed, the hydride reduction of cyclic β-aminoketones has been used extensively to explore the influence of through-bond effects on carbonyl facial selectivity,[9] and elegant work with the aza-adamantanones[9e,f,10] (e.g. **3a**), diaza-adamantanones (e.g. **3b**),[11] and related monoketones[12] have provided among the more compelling illustrations of the Cieplak hyperconjugative transition-state model.[9a] Unexpected reactivity emerges from treatment of **6** (**8** and **9**) with $LiAlH_4$, Red-Al, and DIBAL-H under various conditions—in studies that parallel (in design) those recently performed on a related phloroglucinol-derived natural product[13]—and these results will be reported separately. Of relevance to the current discussion, treatment of **6** with one equivalent of Red-Al provides a modest (33%) yield of the *exo*-mono-reduction

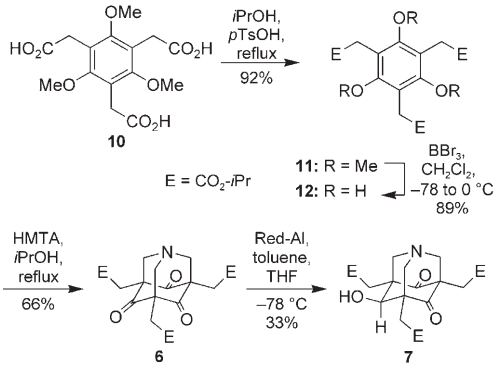

Scheme 1. Synthesis of ester-functionalized 1-aza-adamantanetrione **6** and *exo*-mono-alcohol **7**.

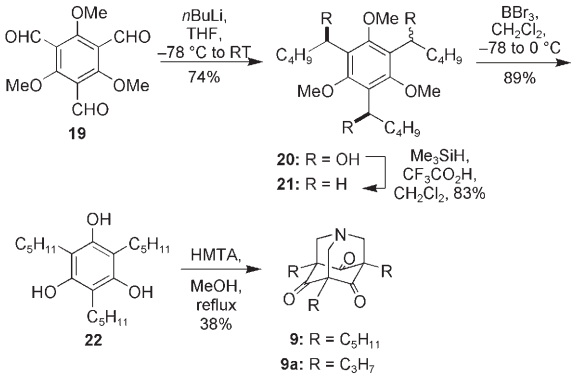

Scheme 3. Synthesis of tripentyl 1-aza-adamantanetrione **9**. Tripropyl **9a**, synthesized by an alternate route, has been reported previously (see ref. [7a]).

product **7** (Scheme 1), in addition to more polar di- and trireduced compounds.

The synthesis of homologated 1-aza-adamantanetrione triester **8** is outlined in Scheme 2. Tribromo scaffold **13**[7a,14] is converted to tripropionic acid **16** using a three-step sequence involving alkylation with diethyl malonate, saponification, and thermally-mediated decarboxylation (78% overall yield for three steps). Fischer esterification then provides **17** in good yield, and a carefully monitored BBr_3-mediated demethylation affords **18**.[8] The Mannich-type cyclization with HMTA provides AAT **8** in 47% yield, when the reaction is again performed in the appropriate alcoholic solvent (*i*PrOH).[15] Triester **8** is found to be readily soluble in common organic solvents.

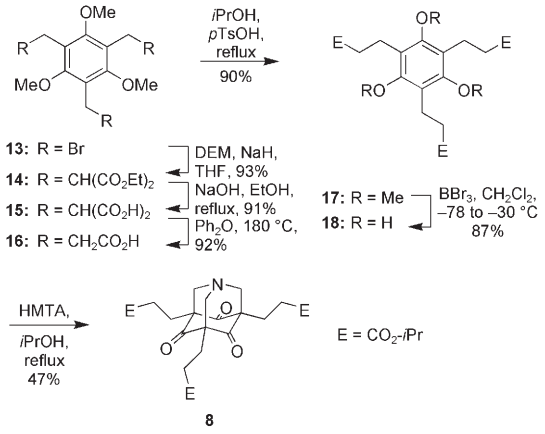

Scheme 2. Synthesis of ester-functionalized 1-aza-adamantanetrione **8**.

Using methodology outlined previously for the exploration of diastereoselective additions to crowded phloroglucinol derivatives,[16] tripentyl AAT **9** is prepared starting from versatile trialdehyde **19**.[17] Three-fold addition of *n*-butyllithium produces triol **20** as a mixture of *anti*,*syn* and *syn*,*syn* isomers (Scheme 3); the mixture is then subjected to trimethylsilyl hydride reduction as described for similar compounds by Biali and co-workers to give **21**.[18] Standard demethylation and HMTA cyclization reactions follow to afford the desired tripentyl AAT **9** (that is somewhat more soluble than previously prepared **9a**[7a]). This procedure appears as our most general one to prepare alkyl- and aryl-substituted AATs.

X-ray crystal structures of 6 and 7—General features and packing: X-ray crystallography is among the best experimental techniques to reveal the structural consequences (e.g., on bond lengths and angles) of hyperconjugative interactions in donor–σ-acceptor molecules.[19] No X-ray structures of the AAT core have been reported in the Cambridge Structural Database (v. 5.28) as of May 2007; only after numerous attempts were we finally able to grow suitable single crystals of **6** (from pentane/ethanol). The asymmetric unit consists of one molecule of **6** and two half ethanol molecules, and the structure is disordered with respect to both components. For the AAT, the disorder is localized in the isopropyl side chains, and could be appropriately modeled in the absence of the solvent. The refined monomer structure is shown in Figure 3a as a stick view and Figure 3b as an ORTEP plot; additional crystallographic details (e.g., parameters, bond lengths, and bond angles) are summarized in the next section as well as the Experimental Section.

The packing structure of **6** is worth mentioning given our interest in the self-assembly of these and related molecules in solution and the solid state. Recognizable is an antiparallel alignment of monomers (Figure 3c), a consequence presumably of favorable dipolar interactions (the calculated ground state dipole of similar AATs is ≈4 D);[7c] the core-to-core distance is ≈6.8 Å. Other intermolecular interactions benefit from this arrangement, including multiple C-H···O contacts[20] (C···O 3.4–3.6 Å) at the interface of the two monomers (e.g. C(10)···O(3)′, O(4)···C(8)′). The cores further organize into layers (Figure 3d, view along the crystallographic *a* axis shown), the result of gentle interactions between the isopropyl side chains at the discernably lipophilic interface. The layer-to-layer distance in this packing motif is ≈11.5 Å.

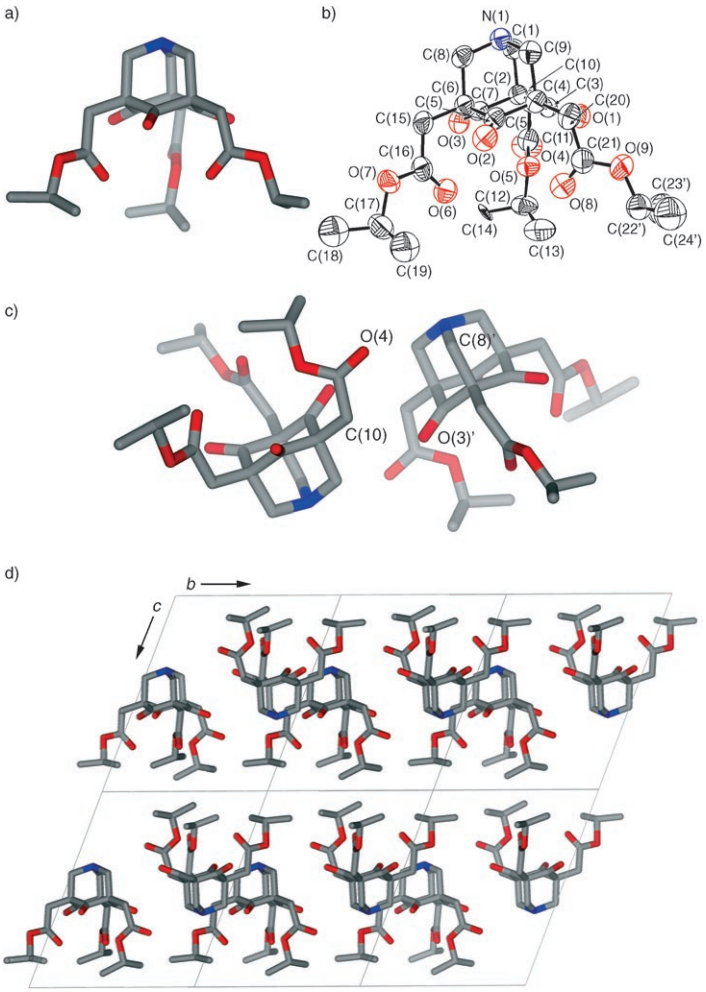

Figure 3. X-ray crystal structure of **6**. a) Monomer structure; solvent molecules and hydrogen atoms have been removed for clarity. b) ORTEP plot where thermal ellipsoids are shown at the 50% probability level. c) Antiparallel alignment of **6** within layers that features multiple C-H···O interactions at the "dimer" interface. d) A packing view (along the *a* axis) showing interaction of the isopropyl side chains at a lipophilic interface. Atom color codes: C = gray, N = blue, O = red.

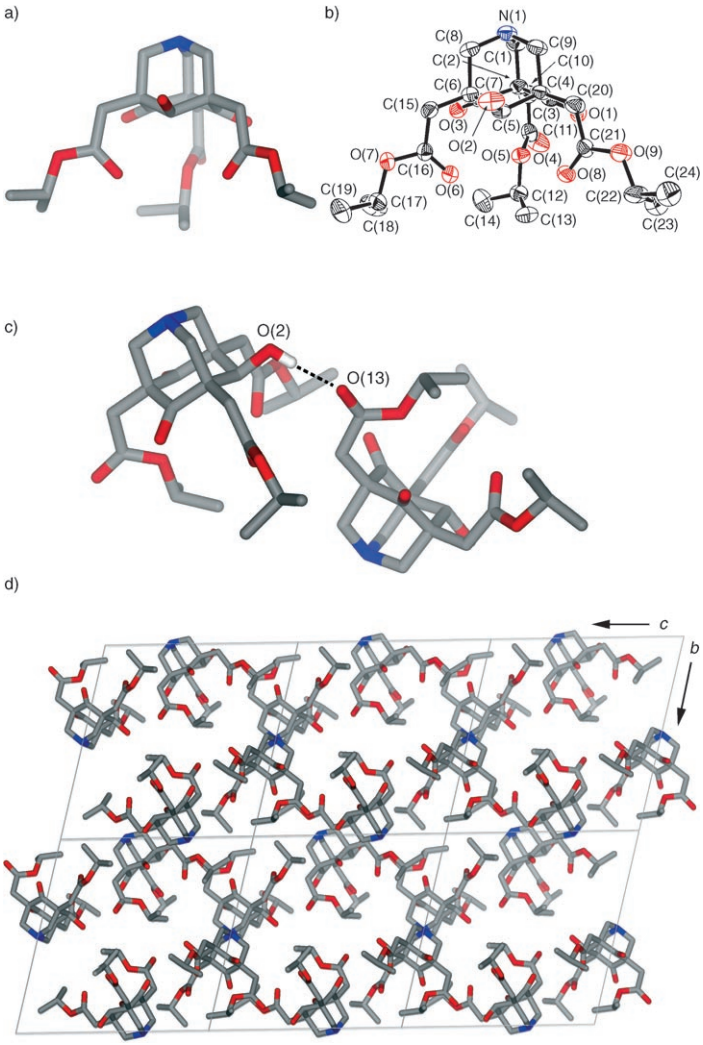

Figure 4. X-ray crystal structure of **7**. a) Monomer structure; solvent molecules and hydrogen atoms have been removed for clarity. b) ORTEP plot where thermal ellipsoids are shown at the 50% probability level. c) Intermolecular hydrogen bonding (indicated by the dashed line) between the *exo* alcohol and neighboring ester carbonyl (O(2)···O(13) = 2.72 Å). d) A packing view (along the *a* axis) showing formation of layers, dominated by side chain interactions. Atom color codes: C = gray, N = blue, O = red.

Alcohol **7** could be recrystallized from a concentrated methylene chloride solution and the refined monomer structure is shown in Figure 4a and b. The asymmetric unit consists of two molecules of **7** (Figure 4c), and three of the six isopropyl side chains are disordered (disorder not shown). The *exo* alcohol participates in a short hydrogen bond with a neighboring ester carbonyl group (O(2)···O(13) = 2.72 Å; O(2)-H···O(13) = 166.7°) in this arrangement. Layers observed by looking along the *a* axis are again dominated by interactions involving the isopropyl side chains (Figure 4d).

The ester side chain conformations displayed by the monomers **6** and **7** in the solid state (Figures 3a and 4a), while certainly influenced by packing of the isopropyl groups, are remarkably similar. The ester C(10)–C(11), C(15)–C(16), and C(20)–C(21) bonds are antiperiplanar to the C_α–C_β bonds (e.g. C(6)–C(8)), and although of "normal" length (average for **6**: 1.497(5) Å; **7**: 1.496(4) Å),[21] stereoelectronics could play a role in stabilizing this conformation. Regardless of the origin, the result for both **6** and **7** is that three of the ester oxygens are positioned underneath the core with an average O···O distance of ≈4.1 Å; whether this space can serve as a binding environment for ions (akin to valinomycin,[22] where O···O ≈4.2 Å for the ester carbonyl oxygens) is currently being evaluated.

Comparative analysis of bond lengths and angles from X-ray structural data: Relevant bond lengths and angles for the monomer structures of **6** and **7** are provided in Table 1 (additional crystallographic data is provided in the Experimental Section); for **7**, data for only one of the molecules in the asymmetric unit is provided and discussed since the values for the two are similar. The comparable monomer

Table 1. Selected bond lengths [Å] and angles [°] for **6** and **7**.[a]

Bond length	**6**	**7**	Angle	**6**	**7**
N(1)−C(1)	1.461(4)	1.442(4)	C(1)-N(1)-C(8)	110.4(3)	110.7(2)
N(1)−C(8)	1.433(4)	1.463(4)	C(1)-N(1)-C(9)	110.6(3)	110.1(2)
N(1)−C(9)	1.451(4)	1.456(4)	C(8)-N(1)-C(9)	111.3(3)	109.3(2)
C(1)−C(2)	1.591(5)	1.591(4)	N(1)-C(1)-C(2)	111.4(3)	112.3(2)
C(4)−C(9)	1.593(5)	1.560(4)	N(1)-C(8)-C(6)	111.5(2)	111.7(2)
C(6)−C(8)	1.598(5)	1.565(3)	N(1)-C(9)-C(4)	111.4(3)	112.5(2)
C(2)−C(3)	1.506(5)	1.520(4)	C(1)-C(2)-C(3)	103.8(3)	104.0(2)
C(3)−C(4)	1.516(5)	1.505(4)	C(1)-C(2)-C(7)	103.3(2)	102.3(2)
C(4)−C(5)	1.515(5)	1.543(4)	C(5)-C(6)-C(8)	103.9(3)	107.8(2)
C(5)−C(6)	1.514(5)	1.540(4)	C(7)-C(6)-C(8)	103.4(2)	103.5(2)
C(6)−C(7)	1.509(5)	1.508(4)	C(3)-C(4)-C(9)	103.7(3)	105.0(2)
C(2)−C(7)	1.513(5)	1.517(4)	C(5)-C(4)-C(9)	103.5(3)	108.0(2)
O(1)−C(3)	1.215(4)	1.213(3)	C(3)-C(4)-C(5)	111.9(3)	109.5(2)
O(2)−C(5)	1.214(4)	1.426(3)	C(5)-C(6)-C(7)	112.4(2)	111.7(2)
O(3)−C(7)	1.224(4)	1.214(3)	C(7)-C(2)-C(3)	112.1(3)	112.2(2)
			C(4)-C(5)-C(6)	114.1(3)	110.3(2)
			C(6)-C(7)-C(2)	114.4(3)	113.9(2)
			C(2)-C(3)-C(4)	114.8(3)	114.2(2)
			C(2)-C(3)-O(1)	122.8(3)	122.1(3)
			C(4)-C(3)-O(1)	121.5(3)	123.4(3)
			C(4)-C(5)-O(2)	122.9(3)	108.4(2)
			C(6)-C(5)-O(2)	122.1(3)	108.5(2)
			C(6)-C(7)-O(3)	122.8(3)	123.1(2)
			C(2)-C(7)-O(3)	122.0(3)	122.1(2)

[a] Standard deviations are shown in parentheses. Additional crystallographic details are provided in the Experimental Section.

conformations of **6** and **7** (Figure 3a and 4a) indeed encourages this side-by-side comparison. Most striking are the long C_α−C_β bonds (i.e., C(1)−C(2), C(4)−C(9), and C(6)−C(8)) of **6**, up to 1.6 Å, that we take a priori as a signature of hyperconjugative interactions. For **7**, equivalent elongation is observed *only* for the C(1)−C(2) bond, the central bond that is flanked by two carbonyl acceptors, highlighting the uniqueness of this arrangement of atoms. Correspondingly, the carbon−carbon bonds for **7** that are not within a donor–σ-acceptor framework (e.g., C(4)−C(5), C(5)−C(6)) appear to be of standard length. Further discussion of bond lengths is best done in the context of similarly strained cyclic molecules (below); indeed, the bond angles within **6** and **7** deviate appreciably from the optimal values (i.e., $\sphericalangle$ C-C-C $\neq$ 109.5°).

Again, the comparison of molecules **6** and **7** to simple structural analogues like **1** or **2** is tempting but would ignore any structural changes associated with ring strain. We have chosen instead to discuss and analyze bond lengths (Figure 5 and Table 2) and angles (Figure 6 and Table 3) in the context of related aza- and deaza-adamantane crystal structures (with crystallographic *R* factors <0.05).[23] Included in Table 2 is the *average* bond length data for **6** and **7**, along side data for analogous structures available in the literature (the di- (CSD code KOLSIN[24]) and mono- (OCAYEW[25]) ketones **23** and **24**, respectively) and a saturated aza-adamantane **25** (EJIQUJ[26]).[27] Also shown are average bond lengths for three adamantanediones (DESVIG (**26**),[28]

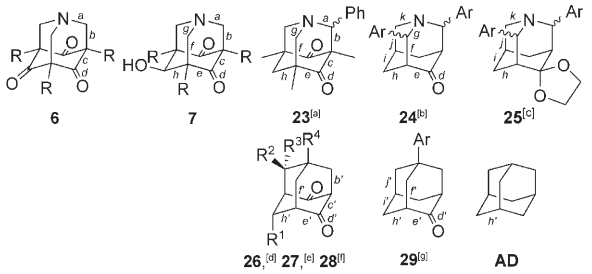

Figure 5. Atom labeling scheme for the bond length data presented in Table 2. R = CH_2CO_2iPr, R^1–R^4 = various substituents, Ph = phenyl, Ar = *p*-nitrophenyl (**24**) or *p*-chlorophenyl (**25**), **AD** = various adamantanes. Reference (CSD code): [a] ref. [24] (KOLSIN); [b] ref. [25] (OCAYEW); [c] ref. [26] (EJIQUJ); [d] ref. [28] (DESVIG); [e] ref. [29] (LIXFIH); [f] ref. [29] (LIXFUT); [g] ref. [30] (FITPED).

Table 2. Comparison of average bond lengths[a] [Å] from the X-ray crystal structures of **6**, **7**, and related tricyclic molecules from Figure 5.

Bond[b]	**6**[c]	**7**[d]	**23**[e]	**24**[f]	**25**[g]	**26**[h], **27**[i], **28**[j]	**29**[k]	**AD**[l]
a	1.45	1.44	1.46	–	–	–	–	–
b, *b*′	1.59	1.59	1.59	–	–	1.55	–	–
c, *c*′	1.51	1.52	1.53	–	–	1.51	–	–
d, *d*′	1.22	1.21	1.21	1.21	–	1.22	1.21	–
e, *e*′	–	1.51	1.50	1.51	–	1.50	1.51	–
f, *f*′	–	1.56	1.54	1.55	–	1.54	1.54	–
g	–	1.46	1.46	1.48	–	–	–	–
h, *h*′	–	1.54	1.53	1.53	1.53	1.54	1.54	1.54
i, *i*′	–	–	–	1.54	1.53	–	1.53	–
j, *j*′	–	–	–	1.53	1.53	–	1.53	–
k	–	–	–	1.47	1.49	–	–	–

[a] The bond lengths for chemically equivalent bonds within each molecule have been averaged. [b] As specified in Figure 5. Crystallographic details (see the Experimental Section for further details of **6** and **7**) including CSD codes and references: [c] **6**: $T=173(2)$ K, $R_1=0.0703$. [d] **7**: $T=173(2)$ K, $R_1=0.0587$. [e] **23** (KOLSIN, Ref. [24]): $T=295$ K, $R_1=0.0470$. [f] **24** (OCAYEW, ref. [25]): $T=293$ K, $R_1=0.0580$. [g] **25** (EJIQUJ, ref. [26]): $T=291$ K, $R_1=0.0456$. [h] **26** (DESVIG, ref. [28]): $T=295$ K, $R_1=0.0490$. [i] **27** (LIXFIH, ref. [29]): $T=295$ K, $R_1=0.0290$. [j] **28** (LIXFUT, ref. [29]): $T=295$ K, $R_1=0.0470$. [k] **29** (FITPED, ref. [30]): $T=295$ K, $R_1=0.0300$. [l] **AD**: various adamantanes from the CSD.

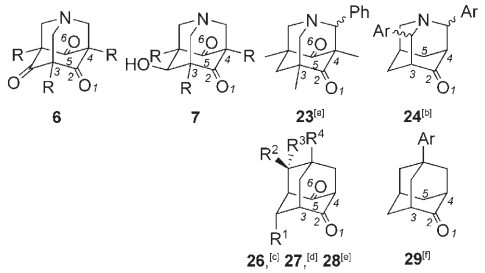

Figure 6. Atom labeling scheme for the bond angle data presented in Table 3. R = CH_2CO_2iPr, R^1-R^4 = various substituents, Ph = phenyl, Ar = *p*-nitrophenyl. Reference (CSD code): [a] ref. [24] (KOLSIN); [b] ref. [25] (OCAYEW); [c] ref. [28] (DESVIG); [d] ref. [29] (LIXFIH); [e] ref. [29] (LIXFUT); [f] ref. [30] (FITPED).

LIXFIH (**27**),[29] and LIXFUT (**28**)[29]), a selected adamantanone (FITPED (**29**)[30]), and variously substituted adamantanes (**AD**). A simplified bond labeling scheme (Figure 5)

Table 3. Comparison of average bond angles[a] [°] from the X-ray crystal structures of **6**, **7**, and related tricyclic molecules from Figure 6.[b]

Angle[c]	**6**	**7**	**23**[d]	**24**[e]	**26**[f]	**27**[g], **28**[h]	**29**[i]
1–2–3	122.3	123.4	123.5	124.1	124.9	124.1	123.7
1–2–4		122.1	121.8	123.2	121.2	122.7	123.9
4–5–6		122.1	121.4	–	121.4	123.1	–
3–2–4	114.4	114.2	114.5	112.7	113.5	112.9	112.3
2–4–5	112.1	112.2	105.8	108.9	105.8	110.5	109.5
Σ_{CNC}	332.3	330.1	330.2	329.4	–	–	–

[a] The bond angles for chemically equivalent bonds within each molecule have been averaged. [b] Standard deviations are shown in parentheses. [c] As specified in Figure 6. CSD codes and references: [d] KOLSIN, ref. [24]. [e] OCAYEW, ref. [25]. [f] DESVIG, ref. [28]. [g] LIXFIH, ref. [29]. [h] LIXFUT, ref. [29]. [i] FITPED, ref. [30].

has been adopted to facilitate the comparison; the letters are kept consistent between structures based on the atom bonding sequence. For example, path *a-b-c-d* uniquely describes the donor–σ-acceptor pathway where central bond *b* is flanked by two carbonyl acceptors.

The analysis reveals somewhat shortened C–N bonds *a* (1.45 Å) versus *k* (1.48 Å), and a considerably elongated C–C bond *b* (1.59 Å) versus *f* (1.55 Å), *j* (1.53 Å), *f′* (1.54 Å), or *j′* (1.53 Å). There is therefore some hint of the bond length alternation that is a classically predicted consequence of hyperconjugation,[2c,31] visualized, if even crudely, by the no-bond resonance structure shown below:

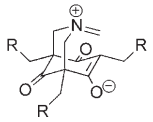

The bond alternation trend does not extend to bonds *c* (1.52 Å versus *e*, *c′*, and *e′* that are all 1.51 Å) or *d* (including *d′*, all C=O bonds are 1.21–1.22 Å). That bond *d* is not substantially perturbed may speak to compensatory stereoelectronic effects in these systems.[32] Comparison of bonds *b′*, *f′*, *h′*, and *j′* (1.53–1.55 Å) reveals only a modest sensitivity to inherent structural changes (and strain) within the deaza-adamantanes; this further implicates donor–acceptor effects in the elongation of bond *b*.

The bond elongation found for *b* (≈0.05 Å) is the largest reported for β-aminoketones; in work by Verhoeven and co-workers with (admittedly less strained) piperidone and tropanone derivatives (bearing carbonyl groups converted to 1,1-dicyanovinyl functions, better electron acceptors), the C_α–C_β bond elongations are ≈0.02 Å and taken as fairly definitive evidence (along with other data) for through-bond interactions. Even so, it seems unnecessary, and likely inappropriate,[31f] to equate the magnitude of the bond length changes to the "strength" of the through-bond interactions in the molecules; suffice it to say, the consequences of donor–acceptor interactions in these aza-adamantanones are detectable. That pathway *a-b-c-d* emerges as unique (one donor nitrogen communicating with two acceptor carbonyls) is analogous to the "enhanced" through-bond effects noted for the diaza-adamantanones like **3b** (that feature two donor nitrogens communicating with one acceptor carbonyl).[5d]

Comparison of selected bond angles of **6** and **7** to those of structural analogues is provided in Figure 6 and Table 3; an arbitrary atom labeling scheme has been adopted for the analysis (Figure 6), which should not be confused with the atom labels reported in the crystallographic data files. There are no significant trends that can be identified for the angles that describe the cyclohexane ring that includes atoms 2–5 across the series. The C–C=O angles (e.g. angle *1–2–3*) fall within 122–125°, and angle *3–2–4* (C–C(=O)–C) is only slightly larger (≈1°) for **6**, **7**, and **23** than for the deaza-adamantanones (but certainly larger than **25** and **AD**, where it is 109–110°). The greatest variation is found at the bridgehead carbon angle, *2–4–5*, although the angle for **6** and **7** is only 1.7° larger than what is found for deaza-analogues **27** and **28**. Based on the sum of the bond angles at nitrogen in the aza-adamantane derivatives, the nitrogen atom of structures **6** and **7** is slightly flattened compared with that of structures **23**, **24**, and **25** ($\Sigma_{C\text{-}N\text{-}C}$ = 328° for **25**); this distortion further aligns the nitrogen lone pair with the C_α–C_β central bond.[19] Without comparing every bond angle for each structure throughout the series, our conclusion is that while **6** and **7** (and **23**) are certainly strained molecules, it is not obvious that their respective bond length changes (in particular elongation of the C_α–C_β bonds) are solely due to this effect. High-level computational studies[33] (e.g. NBO analysis) could shed additional light on the distortions, and these are currently in progress.[34]

Further identified from close inspection of the crystal structures of **6** and **7** is pyramidalization of the carbonyl carbon atoms (labeled *2* in Figure 6).[1c] Similar distortion has been noted by Verhoeven and co-workers in 1,1-dicyanovinyl-modified piperidone and tropanone derivatives.[19,33a] Figure 7 shows one way to report this effect;[33a] namely, as the angle (θ) between the carbonyl vector and the mean plane defined by the three core carbons (*2*, *3*, and *4*). For **6**, θ = 8.7° (the average of three carbonyl groups), and for **7** θ = 7.3° (average of four carbonyl groups, two from each molecule in the asymmetric unit). The largest value reported from Verhoeven's work (recalculated here in the fashion shown in Figure 7) is 6.1°. While the pyramidalization serves to reduce ring strain, that it occurs in such a way (+θ rather than −θ) to further position the carbonyl π bond parallel to the C_α–C_β bonds presumably also optimizes interaction with the nitrogen donor. For **26**, that lacks donor–σ-acceptor interactions, θ = −6.7° for one of the two carbonyl groups (the other features θ ≈0°). Finally, while the sensitivity of the pyramidalization to packing and

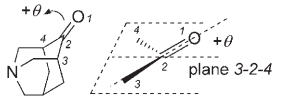

Figure 7. Angle θ, which quantifies the pyramidalization of the carbonyl carbon atoms of **6** and **7**, calculated as the angle between the carbonyl bond and the mean plane defined by carbon atoms 2, 3, and 4.

temperature is not known, it is not reproduced with the same magnitude in the crystal structures of the other molecules shown in Figure 6.

Complementary spectroscopic data: Techniques other than X-ray crystallography have been employed to explore the consequences of donor–acceptor interactions in the rigid aza-adamantanones. Highlighted here is data obtained from UV, IR, and ^{13}C NMR measurements for **6–9**, with some comparative data provided from the literature.

UV spectroscopy is the most routinely used method to diagnose through-bond interactions in β-aminoketones where a new absorption band appears (the lower energy component of a split carbonyl π–π* transition, the so-called σ-coupled transition) to signify communication between the donor and acceptor.[4,5] The absorption data for **6–9** for three solvents is provided in Table 4. A new absorption

Table 4. UV absorption data for **6–9** in different solvents.[a]

Aza-adamantane	λ_{max} [nm]	ε [$M^{-1}cm^{-1}$]	λ_{max} [nm]	ε [$M^{-1}cm^{-1}$]	λ_{max} [nm]	ε [$M^{-1}cm^{-1}$]
	cyclohexane		acetonitrile		ethanol	
6	270	2600	263	3230	265	3010
7	–	–	265	2040	263	1910
8	–	–	267	3270	267	2980
9	271	3060	273	2860	275	3270

[a] Data was collected from 40–120 μM. The absorption intensity was shown to vary linearly with concentration in all cases.

maximum (λ_{max}) is indeed observed in the 260–275 nm window, consistent with (although somewhat red-shifted from) earlier results.[7a,35,36] The frequency deviates little neither with solvent polarity—not surprising given the nominal charge-transfer character of these donor–σ-acceptor molecules[37]—nor peripheral substitution. The molar extinction coefficients, calculated from plots of absorbance versus concentration, are ≈3000 $M^{-1}cm^{-1}$ for the triketones **6**, **8**, and **9**; this value decreases commensurately (i.e., by about one third) for diketone **7**. An identical trend has been reported in related aza-adamantanones[35] and speaks to the participation of all three acceptor carbonyls to the donor–acceptor system. The λ_{max} values do not deviate significantly between the di- and triketones in this work, although a survey of the literature shows that simple (even rigid) β-aminoketones offer values ≈235–245 nm; this increases for the diaza-adamantanones.[4a,5d] Interestingly, the σ-coupled transition can be reversibly abolished[4a] upon protonation by trifluoroacetic acid in acetonitrile (Figure 8; see the Supporting Information for additional details).

IR and ^{13}C NMR spectroscopic data have been used sporadically to report on donor–σ-acceptor interactions and in our estimation interpretation of these data warrants some caution. Notwithstanding the obvious complications of solvation (and experimental conditions in general), differences identified from single-point comparisons (e.g. **1** versus **3**)[5d] are difficult to attribute to any one particular phenomenon,

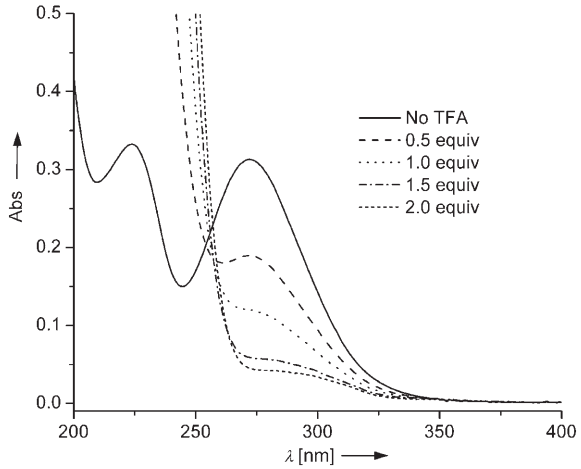

Figure 8. Treatment of a 1.2×10^{-5} M solution of **9** (in acetonitrile) with trifluoroacetic acid (TFA) results in disappearance of the σ-coupled transition.

although this is often done. Additional complication enters when considering IR data for the aza- and deaza-adamantanones bearing two or more ketones in a 1,3-relationship that display Fermi-type coupling;[38] we have used the average carbonyl stretch for making a quick comparison (the complete comparative data, including the data for **6–9**, is provided in the Supporting Information). Across representative adamantanones (two monoketones,[10a,11a,39] two diones,[40,41] and one trione[42]) identified from the literature, the carbonyl stretching frequency is relatively invariant (average value ≈1720 cm^{-1}). A similar consistency is observed for a series of representative aza-adamantanones (including **6–9**),[10a,11a,43] although the analysis reveals a ≈5–20 cm^{-1} shift to lower wavenumber for these donor–σ-acceptor molecules. A similar shift has been identified for the 1,3-diaza-adamantanones (e.g. **3b**).[5d,11a] In some previously reported cases the carbonyl stretch has been restored to higher frequency upon protonation or methylation at nitrogen,[5d,10a] although these experiments have not generally considered structural changes associated with the chemical transformations.[9e,44] The on-average shift to lower energy is consistent with predictions based on through-bond donor–acceptor interactions that would weaken the carbonyl π bond (Figure 1).

A similar treatment of the ^{13}C NMR data for adamantanones and aza-adamantanones reveals, for both series, that the carbonyl resonance shifts upfield as the number of carbonyl groups increases (the complete comparative data, including that of **6–9**, is provided in the Supporting Information). Such a subtle effect does not emerge from the X-ray crystallography data. For example, $\delta_{C=O}$ shifts from ≈218 ppm for adamantanones (in $CDCl_3$),[5e,39,45] to ≈208 ppm for adamantanediones,[46] to ≈202 ppm for adamantanetriones.[42] The aza-adamantanones (including diones and triones) are on-average upfield shifted (≈3–5 ppm) from these values. From monoketone, to dione, to trione the values are δ ≈214 ppm,[5e,11a] 202 ppm (for **7**),[47] and 197–200 ppm, respectively. This trend is again *consistent*

with the hyperconjugative interactions depicted in Figure 1, but such an analysis remains admittedly oversimplified.

Consequences of through-bond interactions on β-aminoketone reactivity—General considerations: When molecules that feature well-characterized donor–acceptor interactions through σ bonds show aberrant chemical behavior the challenge lies in linking the two phenomena. For β-aminoketones, diminished reactivity at nitrogen (basicity/nucleophilicity) is generally taken as a hallmark consequence.[5d,e,h,35,48] Risch and co-workers have shown that the pK_a of the protonated amine of aza-adamantanes decreases by ≈three units upon introduction of each carbonyl acceptor (from ≈10.7 for aza-adamantane to ≈0.3 for aza-adamantanetriones).[35] Likewise, Sasaki and co-workers have noted that the pK_{a1} of protonated diaza-adamantanones like **3b** (≈4–5) is significantly lower than that of aza-adamantanone (8.6[5e]) (or aza-adamantane).[5d] Related studies have shown a diminished nucleophilicity at nitrogen, and some have likened its general reactivity to that of an amide. We found previously[7a] that treatment of **4** with methyl iodide, hydrogen peroxide, or *m*-CPBA gives no reaction at the bridgehead amine (or elsewhere).[49] Through-bond (hyperconjugative) interactions likely play some role in this sluggish reactivity, but general inductive effects[50] in β-aminoketones[48a,51] are also significant; that *N*-methylpiperidine is a much stronger base (pK_b 3.92) than *N*-methylpiperidone (pK_b 6.01)[5e,52] despite "undetectable"[4a,5g] through-bond interactions (e.g. no σ-coupled transition) is evidentiary.

Discussed earlier, through-bond influences on carbonyl reactivity in β-aminoketones have historically been probed through subtle changes in nucleophile addition/hydride reduction stereoselectivity. Molecules **6–9** are complicated substrates for stereochemical analysis given that their carbonyl groups are sterically biased and that some (e.g. **6–8**) bear functional groups capable of metal chelation. Likewise, our own studies[7a] and those of others[5d,43a] note slow or no reaction with conventional carbonyl nucleophiles (e.g. hydrazines, hydroxylamine, diazomethane, alkyl phosphonium ylides, etc.), although these results are difficult to assess (or quantify) in terms of through-bond interactions.

Fragmentation reactions: The orbital arrangement that underlies donor–σ-acceptor interactions in β-aminoketones (Figure 1) is also central to the kinetics and stereoselectivity of Grob fragmentation reactions.[1c,d,53] This connection makes fragmentation studies of the molecules presented here, for which spectroscopic evidence of the intimate relationship between the nitrogen and carbonyl groups has been presented, particularly fitting. Risch and co-workers have elegantly described heterolytic fragmentations of chloro-substituted aza-adamantanones[54] and aza-adamantanediones[55] under basic conditions; an initial report of related reactions of aza-adamantanetriones (i.e. **6**, **8**, and **9**) under acidic conditions is presented below.

Upon treating **6** with dilute acetic acid (HOAc) at 100 °C for 1 h, three distinct products are formed (in ≈98 % combined yield (and ≈1:1:1 molar ratio); Scheme 4) that do not arise from a simple reversal of the Mannich-type cyclization reaction that generates the starting material (Scheme 1). All of the structures were determined by 1D and 2D (gHMBC and gDQCOSY) ^{1}H and ^{13}C NMR analysis using a 500 MHz instrument and confirmed by mass spectrometry. The products include *N*-alkyl-*cis*-3,5-disubstituted piperidone[56] **30** (as a mixture of epimers), isolated in a ≈1:1 molar ratio (determined by integration) with α,β-unsaturated acid **31** after column chromatography (the mixture appears as the higher R_f spot with CH_2Cl_2/MeOH 20:1), and *cis*-3,5-disubstituted piperidone **32** (isolated as the lower R_f spot). To test whether placement of the esters or their presence matters to the products formed (and mechanism), **8** and **9** were subjected to similar conditions. *N*-Alkyl-*cis*-3,5-disubstituted piperidones **33** (69 % yield, again as a mixture of epimers) and **34** (≈75 % yield) could be isolated from the reaction of **8** and **9**, respectively. In both cases a small amount (< 5 %) of the alkenes (**35** and **36**) were also identified by NMR. The reactions appear to share a common mechanism that is specific to the AAT core.

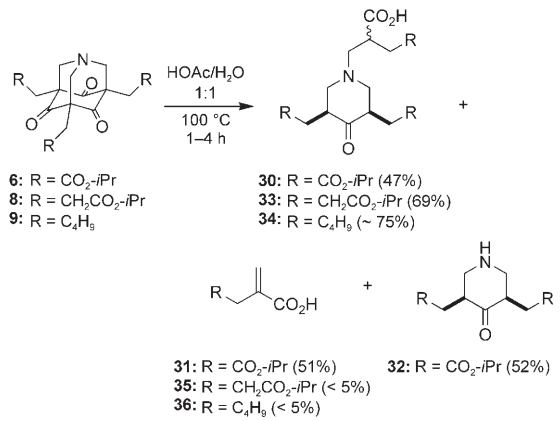

Scheme 4. Acid-mediated fragmentation reactions of aza-adamantanetriones **6**, **8**, and **9**.

Scheme 5 shows a proposed mechanism to rationalize the fragmentation products. We favor a first productive step of carbonyl protonation followed by hydration to form **A**, a process already discussed for aza-adamantanetriones under aqueous acidic conditions.[35] The resulting hydrate can then collapse to the diketo-acid intermediate **B** through a retro-Claisen-like process. A similar mechanistic sequence could then repeat; carbonyl protonation and hydration of **B**, followed by fragmentation of the core and thermally-mediated decarboxylation to afford the *N*-alkyl-*cis*-3,5-disubstituted piperidones (**30**, **33**, and **34**). The increased nitrogen basicity of **B** (relative to the starting material)[35] makes protonation here plausible; this initiates an alternative hydration/fragmentation/decarboxylation pathway that could account for the formation of piperidone **32** and α,β-unsaturated acid **31** (and **35**/**36** for **8**/**9**). That the alkene **31** does not come directly from **30** has been proven by subjecting pure **30** to the

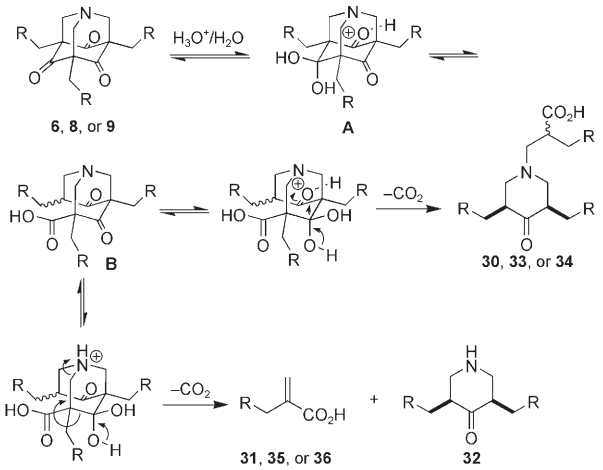

Scheme 5. Proposed mechanistic pathway for the acid-mediated fragmentation of **6**, **8**, and **9**.

reaction conditions and monitoring its stability by ^{1}H NMR (over four hours). Future work could consider this methodology as a general way to prepare highly substituted *cis*-3,5-disubstituted piperidones, important building blocks in the synthesis of alkaloids and analgesics.[57]

Conclusion

A combination of experimental techniques and comparative analysis has shown that the through-bond donor–acceptor interactions in appropriately functionalized β-aminoketones can be particularly assessable. Uniquely for the 1-aza-adamantanones, molecules in which the donor and acceptor orientation is permanently optimized, many of the hallmark consequences of through-bond communication emerge. These include elongation of the central C–C bond in the donor–σ-acceptor pathway (to ≈1.6 Å), the presence of a new absorption band in the molecules′ UV/Vis spectra, and IR/^{13}C NMR spectroscopic shift trends (versus similarly strained molecules that lack either the donor or acceptor groups) consistent with theoretical expectations. The arrangement of donor and acceptor groups has functional consequences as well in terms of the molecules′ reactivity profiles.

We previously showed that molecules like **4** and **5** self-assemble in solution and that the emergent macromolecular properties respond to molecular-level changes that also influence the donor–σ-acceptor interactions. The current molecular-level analysis that finds pronounced structural, spectroscopic, and reactivity consequences for traditionally weak effects suggests that they have been largely overlooked on the supramolecular scale where similarly modest interactions are often amplified. Left now is to introduce these donor–σ-acceptor arrangements into macromolecules, where even the simplest motifs could offer ways to tune bulk properties not available to more traditional weak interactions.

Experimental Section

Materials and general methods: Reagents and solvents were purchased from commercial sources and used without further purification unless otherwise specified. THF, ether, CH_2Cl_2, and DMF were degassed in 20 L drums and passed through two sequential purification columns (activated alumina; molecular sieves for DMF) under a positive argon atmosphere. Thin layer chromatography (TLC) was performed on SiO_2–60 F_{254} aluminum plates with visualization by UV light or staining. Flash column chromatography was performed using Purasil SiO_2–60, 230–400 mesh from Whatman. Melting points (m.p.) were determined on a Mel-temp electrothermal melting point apparatus and are uncorrected. 300 (75) MHz and 500 (125) MHz ^{1}H (^{13}C) NMR spectra were recorded on Varian Mercury 300, Gemini 300, VXR 300, and Varian Inova (500) spectrometers. Chemical shifts (δ) are given in parts per million (ppm) relative to TMS and referenced to residual protonated solvent ($CDCl_3$: δ_H 7.27 ppm, δ_C 77.00 ppm; [D_6]DMSO: δ_H 2.50 ppm, δ_C 39.50 ppm). Abbreviations used are s (singlet), d (doublet), t (triplet), q (quartet), quin (quintet), hp (heptet), b (broad), and m (multiplet). UV/Vis absorption spectra were obtained using a Cary 100 Bio spectrophotometer and 1 cm quartz cells. ESI- and ESI-TOF-MS spectra were recorded on a Bruker APEX II FTICR and Agilent 6210 TOF spectrometer, respectively. EI-, CI-, and DIP-CI-MS spectra were recorded on a Thermo Trace GC DSQ (single quadrupole) spectrometer. The syntheses of **8**, **9**, **13**–**22**, and **30**–**35** as well as ^{1}H and ^{13}C NMR spectra for all new compounds are presented in the Supporting Information.

X-ray crystal structure determination and refinement: Data were collected at 173 K on a Siemens SMART PLATFORM equipped with a CCD area detector and a graphite monochromator utilizing $Mo_{K\alpha}$ radiation ($\lambda = 0.71073$ Å). Cell parameters were refined using up to 8192 reflections. A full sphere of data (1850 frames) was collected using the ω-scan method (0.3° frame width). The first 50 frames were re-measured at the end of data collection to monitor instrument and crystal stability (maximum correction on I was $< 1\%$). Absorption corrections by integration were applied based on measured indexed crystal faces. The structure was solved by the Direct Methods in SHELXTL6,[58] and refined using full-matrix least squares on F^2. The non-H atoms were treated anisotropically, whereas the hydrogen atoms were calculated in ideal positions and were riding on their respective carbon atoms. Details are provided in Table 5. For **6**, the asymmetric unit consists of the molecule and two half ethanol

Table 5. Crystal data and structure refinement for **6** and **7**.

	6	**7**
empirical formula	$C_{26}H_{39}NO_{10}$	$C_{24}H_{35}NO_9$
formula weight	525.58	481.53
crystal system	triclinic	triclinic
space group	$P\bar{1}$	$P\bar{1}$
a [Å]	11.4801(16)	12.7729(16)
b [Å]	11.6917(16)	14.7468(18)
c [Å]	13.3142(19)	14.8080(18)
α [°]	104.663(3)	75.036(2)
β [°]	97.753(2)	73.265(2)
γ [°]	116.825(2)	84.410(2)
V [Å^3]	1477.2(4)	2579.7(5)
Z	2	4
ρ_{calcd} [g cm^{-3}]	1.182	1.240
crystal size [mm^3]	0.18×0.17×0.05	0.26×0.19×0.11
independent reflections	3871	9042
observed reflections [$I > 2\sigma(I)$]	2736	5600
index ranges	$-12 \le h \le 12$	$-15 \le h \le 9$
	$-12 \le k \le 10$	$-17 \le k \le 17$
	$-14 \le l \le 14$	$-17 \le l \le 16$
parameters	314	628
$F(000)$	564	1032
goodness-of-fit (on F^2)	1.051	1.034
R_1 based on F [$I > 2\sigma(I)$]	0.0703	0.0587
wR_2 based on F [$I > 2\sigma(I)$]	0.2079	0.1325

molecules; each disordered around an inversion center. The latter were disordered and could not be modeled properly, thus the program SQUEEZE,[59] a part of the PLATON package[60] of crystallographic software, was used to calculate the solvent disorder area and remove its contribution to the overall intensity data.

CCDC 656392 (**6**) and 656393 (**7**) contain the supplementary crystallographic data for this paper. These data can be obtained free of charge from The Cambridge Crystallographic Data Centre via www.ccdc.cam.ac.uk/data_request/cif.

Isopropyl 2,2′,2″-(2,4,6-trimethoxybenzene-1,3,5-triyl)triacetate (11): *p*TsOH·H_2O (1.13 g, 5.92 mmol) was added to a stirred solution of triacid **10**[7b] (0.900 g, 2.63 mmol) in isopropanol (25 mL) and the reaction was heated under reflux overnight. All volatiles were then removed under reduced pressure and the residue was taken up with EtOAc and washed with dilute NaOH. The organic solution was then dried over $MgSO_4$ and concentrated under reduced pressure and the residue was purified using column chromatography (hexanes/EtOAc 3:1) to afford **11** (1.13 g, 92%) as a colorless oil. ^{1}H NMR (300 MHz, $CDCl_3$): δ = 1.23 (d, ^3J = 6.3 Hz, 18H), 3.63 (s, 6H), 3.72 (s, 9H), 5.05 ppm (m, ^3J = 6.3 Hz, 3H); ^{13}C NMR (75 MHz, $CDCl_3$): δ = 21.7, 30.8, 61.2, 68.0, 118.6, 157.7, 171.5 ppm; MS (EI): *m*/*z*: calcd for $C_{24}H_{36}O_9$: 468.2359; found 468.2355 $[M]^+$.

Isopropyl 2,2′,2″-(2,4,6-trihydroxybenzene-1,3,5-triyl)triacetate (12): BBr_3 (1.26 mL, 13.3 mmol) was added at −78 °C to a stirred solution of **11** (1.04 g, 2.22 mmol) in dry dichloromethane (60 mL) and the resulting reaction mixture was stirred for 2 h before warming to 0 °C for 20 min. The reaction was then quenched with saturated aqueous $NaHCO_3$, poured into a separatory funnel, and extracted with dichloromethane (3× 50 mL). The organics were combined, dried over $MgSO_4$ and concentrated under reduced pressure to afford a crude solid. Purification by column chromatography (hexanes/EtOAc 3:1) gave **12** (0.85 g, 89%) as a colorless solid. M.p. 163–164 °C; ^{1}H NMR (300 MHz, $CDCl_3$): δ = 1.28 (d, ^3J = 6.6 Hz, 18H), 3.76 (s, 6H), 5.03 (m, ^3J = 6.3 Hz, 3H), 8.50 ppm (s, 3H); ^{13}C NMR (75 MHz, $CDCl_3$): δ = 21.6, 30.6, 69.9, 103.0, 153.8, 175.3 ppm; MS (EI): *m*/*z*: calcd for $C_{21}H_{30}O_9$: 426.1890, found 426.1879 $[M]^+$.

2,5,7-Tris-(2-isopropoxycarbonylmethyl)-1-aza-adamantane-4,6,10-trione (6): Hexamethylenetetramine (0.270 g, 1.93 mmol) was added to a solution of **12** (0.820 g, 1.93 mmol) in isopropanol (15 mL) and the reaction mixture was heated to reflux for 20 h. After cooling to RT, all volatiles were removed under reduced pressure. The residue was purified by column chromatography (hexanes/EtOAc 3:2) to afford **6** (0.61 g, 66%) of a colorless solid. M.p. 111–112 °C; ^{1}H NMR (300 MHz, $CDCl_3$): δ = 1.22 (d, ^3J = 6.0 Hz, 18H), 2.73 (s, 6H), 3.76 (s, 6H), 4.99 (hp, ^3J = 6.0 Hz, 3H); ^{13}C NMR (75 MHz, $CDCl_3$): δ = 21.6, 32.0, 68.2, 70.3, 70.8, 169.0, 197.2 ppm; IR (KBr): $\tilde{\nu}$ = 2984, 2924, 2853, 1731, 1700, 1191, 1109, 798 cm^{-1}; UV/Vis (ethanol): λ_{max} (ε) = 265 nm (3010); MS (EI): *m*/*z*: calcd for $C_{24}H_{33}NO_9$: 479.2155; found 479.2159 $[M]^+$.

2,5,7-Tris-(2-isopropoxycarbonylmethyl)-10-*exo*-hydroxy-1-aza-adamantane-4,6-dione (7): Ester **6** (0.180 g, 0.376 mmol) was dissolved in dry THF (15 mL) and cooled to −78 °C under argon. To this solution was slowly added Red-Al (0.376 mmol, 0.28 mL, 65 wt% in toluene). The solution temperature was maintained at −78 °C until the starting material was consumed (30 min), and then the reaction was quenched with dilute HCl. The resulting mixture was warmed to RT and the solvent was removed in vacuo. The residue was redissolved in EtOAc, washed with water and brine, dried over $MgSO_4$, and concentrated in vacuo. Column chromatography (hexanes/EtOAc 2:1→1:1) afforded **7** (60 mg, 33%) as a white solid. M.p. 139–140 °C; ^{1}H NMR (300 MHz, $CDCl_3$): δ = 1.22 (m, 18H), 2.48 (d, ^3J = 15.9 Hz, 2H), 2.56 (d, ^3J = 15.9 Hz, 2H), 2.62 (s, 2H), 2.98 (d, ^3J = 12.6 Hz, 2H), 3.54 (s, 2H), 3.53 (s, 1H), 3.80 (d, ^3J = 12.9 Hz, 2H), 4.52 (s, 1H), 4.98 ppm (m, 3H); ^{13}C NMR (75 MHz, $CDCl_3$): δ = 21.6, 21.7, 31.7, 34.6, 54.8, 59.2, 68.0, 68.3, 68.7, 69.9, 71.1, 169.7, 170.9, 201.7 ppm; IR (KBr): $\tilde{\nu}$ = 3467, 2981, 2936, 2877, 1726, 1697, 1374, 1195, 1109, 823 cm^{-1}; UV/Vis (ethanol): λ_{max} (ε) = 263 nm (1910); MS (EI): *m*/*z*: calcd for $C_{24}H_{35}NO_9$: 481.2312; found 481.2298 $[M]^+$.

2-(((*syn*)-3,5-Di(2-isopropoxy-2-oxoethyl)-4-oxopiperidin-1-yl)methyl)-4-isopropoxy-4-oxobutanoic acid (30): A solution of **6** (0.250 g, 0.522 mmol) in HOAc/H_2O 1:1 (16 mL) was heated under reflux for 1 h. The solvent was then removed with reduced pressure and the residue was purified by flash chromatography (CH_2Cl_2/MeOH 20:1) to afford a mixture of **30** (0.115 g, 47%) and **31** (0.046 g, 51%) as a colorless oil, and **32** (0.081 g, 52%) as a colorless solid. ^{1}H NMR (500 MHz, $CDCl_3$): δ = 1.16 (m, 18H), 2.12 (dd, ^3J = 16.9, 6.1 Hz, 1H), 2.13 (dd, ^3J = 17.0, 6.2 Hz, 1H), 2.40 (t, ^3J = 11.8 Hz, 1H), 2.44 (dd, ^3J = 16.8, 6.2 Hz, 1H), 2.48 (t, ^3J = 11.7 Hz, 1H), 2.60 (m, 1H), 2.64 (m, 1H), 2.70 (dd, ^3J = 13.2, 6.0 Hz, 1H), 2.74 (dd, ^3J = 17.3 Hz, 7.0 Hz, 1H), 2.90 (dd, ^3J = 12.1, 10.2 Hz, 1H), 3.02 (dq, ^3J = 9.8 Hz, 6.5 Hz, 1H), 3.15 (dq, ^3J = 11.2, 5.8 Hz, 1H), 3.18 (dq, ^3J = 11.9, 5.8 Hz, 1H), 3.31 (ddd, ^3J = 11.3, 6.1 Hz, 2.3 Hz, 1H), 3.43 (ddd, ^3J = 11.6, 6.0, 2.7 Hz, 1H), 4.93 (m, 3H), 10.63 ppm (s, 1H); ^{13}C NMR (125 MHz, $CDCl_3$): δ = 22.0, 32.0, 34.1, 38.6, 44.8, 45.0, 57.3, 57.8, 58.8, 68.5, 170.5, 171.5, 176.7, 206.4 ppm; MS (ESI): *m*/*z*: calcd for $C_{23}H_{38}NO_9$: 472.2541; found 472.2525 $[M+H]^+$.

4-Isopropoxy-2-methylene-4-oxobutanoic acid (31): ^{1}H NMR (500 MHz, $CDCl_3$): δ = 1.16 (m, 6H), 3.23 (s, 2H), 4.93 (m, 1H), 5.72 (s, 1H), 6.34 (s, 1H), 10.63 ppm (s, 1H); ^{13}C NMR (125 MHz, $CDCl_3$): δ = 22.0, 37.9, 68.5, 130.2, 134.2, 170.5, 171.1 ppm; MS (ESI): *m*/*z*: calcd for $C_8H_{13}O_4$: 173.0808; found 173.0801 $[M+H]^+$.

***syn*-Isopropyl 2,2′-(4-oxopiperidine-3,5-diyl)diacetate (32)**: ^{1}H NMR (500 MHz, $CDCl_3$): δ = 1.16 (m, 12H), 2.08 (dd, ^3J = 17.1, 6.8 Hz, 2H), 2.62 (t, ^3J = 12.2 Hz, 2H), 2.66 (dd, ^3J = 16.9, 6.1 Hz, 2H), 3.01 (dq, ^3J = 12.3, 6.1 Hz, 2H), 3.48 (dd, ^3J = 12.6, 6.0 Hz, 2H), 4.92 (hp, ^3J = 5.9 Hz, 2H), 5.88 ppm (s, 1H); ^{13}C NMR (125 MHz, $CDCl_3$): δ = 22.0, 31.9, 48.2, 52.6, 68.3, 171.5, 207.2 ppm; MS (CI): *m*/*z*: calcd for $C_{15}H_{26}NO_5$: 300.1811; found 300.1829 $[M+H]^+$.

Acknowledgements

This work was financially supported by the National Science Foundation CAREER program (CHE-0548003) and the University of Florida. A.J.L. was supported by a University of Florida Alumni Graduate Fellowship and A.A. by the National Science Foundation REU program (CHE-0353828). K.A.A. thanks the National Science Foundation and University of Florida for funding the X-ray crystallography equipment.

[1] a) R. Hoffmann, A. Imamura, W. J. Hehre, *J. Am. Chem. Soc.* **1968**, *90*, 1499–1509; b) R. Hoffmann, *Acc. Chem. Res.* **1971**, *4*, 1–9; c) R. Gleiter, W. D. Stohrer, R. Hoffmann, *Helv. Chim. Acta* **1972**, *55*, 893–906; d) R. Gleiter, *Angew. Chem.* **1974**, *86*, 770–775; *Angew. Chem. Int. Ed. Engl.* **1974**, *13*, 696–701; e) M. N. Paddon-Row, *Acc. Chem. Res.* **1982**, *15*, 245–251; f) R. Gleiter, W. Schafer, *Acc. Chem. Res.* **1990**, *23*, 369–375.

[2] For excellent leading references on hyperconjugation see: a) J. B. Lambert, Y. Zhao, R. W. Emblidge, L. A. Salvador, X. Liu, J.-H. So, E. C. Chelius, *Acc. Chem. Res.* **1999**, *32*, 183–190; b) I. V. Alabugin, T. A. Zeidan, *J. Am. Chem. Soc.* **2002**, *124*, 3175–3185; c) I. V. Alabugin, M. Manoharan, *J. Org. Chem.* **2004**, *69*, 9011–9024.

[3] This nomenclature designates the amine (lone pair, n orbital) as the donor and the carbonyl (π* orbital) as the acceptor, although the orbital interactions are even more complex (e.g. $n \rightarrow \sigma^*_{C-C}$, $\sigma \rightarrow \pi^*_{C=O}$, etc.).

[4] a) R. C. Cookson, J. Henstock, J. Hudec, *J. Am. Chem. Soc.* **1966**, *88*, 1060–1062; b) R. C. Cookson, *Proc. R. Soc. London Ser. A* **1967**, *297*, 27–39.

[5] a) J. Kuthan, J. Palecek, *Collect. Czech. Chem. Commun.* **1963**, *28*, 2260–2264; b) W. A. Ayer, B. Altenkir, R. H. Burnell, M. Moinas, *Can. J. Chem.* **1969**, *47*, 449–455; c) J. Hudec, *J. Chem. Soc. Chem. Commun.* **1970**, 829–831; d) T. Sasaki, S. Eguchi, T. Kiriyama, Y. Sakito, *J. Org. Chem.* **1973**, *38*, 1648–1652; e) A. W. J. Dekkers, J. W. Verhoeven, W. N. Speckamp, *Tetrahedron* **1973**, *29*, 1691–1696; f) P. Pasman, J. W. Verhoeven, T. J. Deboer, *Tetrahedron* **1976**, *32*, 2827–2830; g) A. M. Halpern, A. L. Lyons, *J. Am. Chem. Soc.* **1976**, *98*, 3242–3247; h) J. R. Wiseman, H. O. Krabbenhoft, R. E. Lee, *J. Org. Chem.* **1977**, *42*, 629–632; i) J. W. Verhoeven, in *Electron Transfer-from Isolated Molecules to Biomolecules, Pt. 1, Vol. 106* (Eds.: J. Jortner, M. Bixon), **1999**, pp. 603–644.

[6] N. Risch, *J. Chem. Soc. Chem. Commun.* **1983**, 532–533.
[7] a) H. Li, E. A. Homan, A. J. Lampkins, I. Ghiviriga, R. K. Castellano, *Org. Lett.* **2005**, *7*, 443–446; b) A. J. Lampkins, O. Abdul-Rahim, H. Li, R. K. Castellano, *Org. Lett.* **2005**, *7*, 4471–4474; c) B. G. Sumpter, V. Meunier, A. Vázquez-Mayagoitia, R. K. Castellano, *Int. J. Quantum Chem.* **2007**, *107*, 2233–2242; d) B. G. Sumpter, V. Meunier, E. F. Valeev, A. J. Lampkins, H. Li, R. K. Castellano, *J. Phys. Chem. C* in press.
[8] Notably, treatment of triester-functionalized phloroglucinol derivatives with Lewis or protic acids results, under certain conditions, in significant lactone formation. We are exploring this chemistry separately and will report on it in due course.
[9] See a special issue on diastereoselectivity: a) A. S. Cieplak, *Chem. Rev.* **1999**, *99*, 1265–1336; b) W. Adcock, N. A. Trout, *Chem. Rev.* **1999**, *99*, 1415–1435; c) S. Tomoda, *Chem. Rev.* **1999**, *99*, 1243–1263; d) G. Mehta, J. Chandrasekhar, *Chem. Rev.* **1999**, *99*, 1437–1467; e) B. W. Gung, *Chem. Rev.* **1999**, *99*, 1377–1386; f) M. Kaselj, W. S. Chung, W. J. le Noble, *Chem. Rev.* **1999**, *99*, 1387–1413.
[10] a) J. M. Hahn, W. J. le Noble, *J. Am. Chem. Soc.* **1992**, *114*, 1916–1917; b) E. M. Gonikberg, W. J. le Noble, *J. Org. Chem.* **1995**, *60*, 7751–7755; c) B. W. Gung, *Tetrahedron* **1996**, *52*, 5263–5301; d) M. Kaselj, E. M. Gonikberg, W. J. le Noble, *J. Org. Chem.* **1998**, *63*, 3218–3223; e) S. Tomoda, T. Senju, *Tetrahedron* **1999**, *55*, 5303–5318.
[11] a) Y. Senda, M. Morita, H. Itoh, *J. Chem. Soc. Perkin Trans. 2* **1996**, 221–224; b) Y. Senda, *Chirality* **2002**, *14*, 110–120.
[12] a) J. M. Coxon, K. N. Houk, R. T. Luibrand, *J. Org. Chem.* **1995**, *60*, 418–427; b) V. Yadav, G. Senthil, D. Jeyaraj, *Tetrahedron* **1999**, *55*, 14211–14218; c) F. Jimenez-Cruz, R. Cetina, H. Rios-Olivares, *Chem. Lett.* **2000**, 956–957; d) D. Moraleda, C. Ollivier, M. Santelli, *Tetrahedron Lett.* **2006**, *47*, 5471–5474.
[13] L. Verotta, O. Sterner, G. Appendino, E. Bombardelli, T. Pilati, *Eur. J. Org. Chem.* **2006**, 5479–5484.
[14] B. R. Cho, K. Chajara, H. J. Oh, K. H. Son, S.-J. Jeon, *Org. Lett.* **2002**, *4*, 1703–1706.
[15] When the cyclization is performed in methanol, the triisopropyl ester (20%) is obtained in addition to two of the three possible methyl ester derivatives (the mono-, 21%, and bis-methylester, 6%).
[16] A. J. Lampkins, O. Abdul-Rahim, R. K. Castellano, *J. Org. Chem.* **2006**, *71*, 5815–5818.
[17] B. W. Domagalska, L. Syper, K. A. Wilk, *Tetrahedron* **2004**, *60*, 1931–1939.
[18] S. Simaan, J. S. Siegel, S. E. Biali, *J. Org. Chem.* **2003**, *68*, 3699–3701.
[19] a) B. Krijnen, H. B. Beverloo, J. W. Verhoeven, C. A. Reiss, K. Goubitz, D. Heijdenrijk, *J. Am. Chem. Soc.* **1989**, *111*, 4433–4440; b) D. J. A. De Ridder, K. Goubitz, H. Schenk, B. Krijnen, J. W. Verhoeven, *Helv. Chim. Acta* **2003**, *86*, 799–811; c) D. J. A. De Ridder, K. Goubitz, H. Schenk, B. Krijnen, J. W. Verhoeven, *Helv. Chim. Acta* **2003**, *86*, 812–826.
[20] R. K. Castellano, *Curr. Org. Chem.* **2004**, *8*, 845–865.
[21] Compared with similar isopropyl ester substituents in the CSD (HEFKOS10 = 1.508 Å; HEFKUY10 = 1.509 Å).
[22] J. P. Degelaen, P. Pham, E. R. Blout, *J. Am. Chem. Soc.* **1984**, *106*, 4882–4890.
[23] The X-ray structures of **6** and **7** have been collected at 173 K, while those taken from the literature for comparison have generally been collected at room temperature (290–295 K). The consequence of temperature on through-bond interactions in these systems (in the solid state) is not known.
[24] N. Risch, M. Langhals, W. Mikosch, H. Bögge, A. Müller, *J. Am. Chem. Soc.* **1991**, *113*, 9411–9412.
[25] F. Jiménez-Cruz, R. Cetina-Rosado, S. Hernández-Ortega, R. A. Toscano, H. Ríos-Olivares, *Acta Crystallogr. Sect. C* **2001**, *57*, 868–869.
[26] F. Jiménez-Cruz, H. Ríos-Olivares, S. Hernández-Ortega, A. Cervantes-Nevarez, *J. Mol. Struct.* **2003**, *655*, 23–29.
[27] Side-by-side analysis of some structures is complicated by substitution α to the nitrogen, although comparison to similarly substituted aza-adamantanes suggests that the substituents should have a marginal effect on the bond lengths and angles of the core. Reference [24] states for **23** that "the deformation of the tricyclic system induced by the incorporation of the phenyl ring is quite small."
[28] P. W. Hickmott, M. G. Ahmed, S. A. Ahmed, S. Wood, M. Kapon, *J. Chem. Soc. Perkin Trans. 1* **1985**, 2559–2571.
[29] M. G. Ahmed, S. M. I. Moeiz, S. A. Ahmed, F. Kiuchi, Y. Tsuda, P. Sampson, *J. Chem. Res. Synop.* **1999**, 316–317.
[30] V. A. Tafeenko, A. E. Prozorovskii, V. V. Kovalev, I. V. Knyazeva, *J. Struct. Chem.* **1987**, *28*, 155–158.
[31] a) D. A. Dougherty, W. D. Hounshell, H. B. Schlegel, R. A. Bell, K. Mislow, *Tetrahedron Lett.* **1976**, *17*, 3479–3482; b) D. A. Dougherty, H. B. Schlegel, K. Mislow, *Tetrahedron* **1978**, *34*, 1441–1447; c) E. Osawa, P. M. Ivanov, C. Jaime, *J. Org. Chem.* **1983**, *48*, 3990–3993; d) D. A. Dougherty, C. S. Choi, G. Kaupp, A. B. Buda, J. M. Rudzinski, E. Osawa, *J. Chem. Soc. Perkin Trans. 2* **1986**, 1063–1070; e) N. L. Allinger, K. S. Chen, J. A. Katzenellenbogen, S. R. Wilson, G. M. Anstead, *J. Comput. Chem.* **1996**, *17*, 747–755; f) K. K. Baldridge, T. R. Battersby, R. VernonClark, J. S. Siegel, *J. Am. Chem. Soc.* **1997**, *119*, 7048–7054.
[32] V. Galasso, *THEOCHEM* **2000**, *528*, 171–176.
[33] a) A. M. Brouwer, B. Krijnen, *J. Org. Chem.* **1995**, *60*, 32–40; b) W. D. Oosterbaan, R. W. A. Havenith, C. A. van Walree, L. W. Jenneskens, R. Gleiter, H. Kooijman, A. L. Spek, *J. Chem. Soc. Perkin Trans. 2* **2001**, 1066–1074.
[34] Worth noting, DFT-LDA/cc-pVDZ calculations already performed on **4** (and reported in ref. [7c]) show bond lengths and angles for the AAT core that agree very well with those reported herein (generally within 0.01 Å and 1.5°, respectively). Calculations at the molecular mechanics level (e.g. Amber* force field) do not reproduce the bond length changes, a phenomenon noted in ref. [31e] but argued against in ref. [31f].
[35] D. Kardel, W. Knoche, N. Risch, *J. Chem. Soc. Perkin Trans. 2* **1993**, 1455–1459.
[36] The n–π* transition is too weak to be observed in these systems (see related results in ref. [5d]).
[37] This is not the case for through-bond interactions that show marked charge-transfer character. See, for example, ref. [19].
[38] Cooperative stretching of the carbonyls in these systems has been noted before (see below, ref. [43a]), but we could not find any references of a comprehensive study or discussion.
[39] D. A. Lightner, T. D. Bouman, W. M. Donald Wijekoon, A. E. Hansen, *J. Am. Chem. Soc.* **1984**, *106*, 934–944.
[40] D. Lenoir, P. Mison, E. Hyson, P. v. R. Schleyer, M. Saunders, P. Vogel, L. A. Telkowski, *J. Am. Chem. Soc.* **1974**, *96*, 2157–2164.
[41] R. K. Murray, Jr., D. L. Goff, T. M. Ford, *J. Org. Chem.* **1977**, *42*, 3870–3874.
[42] G. E. Henry, H. Jacobs, C. M. S. Carrington, S. McLean, W. F. Reynolds, *Tetrahedron Lett.* **1996**, *37*, 8663–8666.
[43] a) N. Risch, *Chem. Ber.* **1985**, *118*, 4849–4856; b) N. Risch, U. Billerbeck, E. Krieger, *Chem. Ber.* **1992**, *125*, 459–465.
[44] B. W. Gung, M. A. Wolf, *J. Org. Chem.* **1996**, *61*, 232–236.
[45] J. M. Grill, J. W. Ogle, S. A. Miller, *J. Org. Chem.* **2006**, *71*, 9291–9296.
[46] H. Duddeck, V. Wiskamp, D. Rosenblum, *J. Org. Chem.* **1981**, *46*, 5332–5336.
[47] The average value for 1-aza-adamantanediones from ref. [43a] is $\delta \approx 207$ ppm. Such an NMR comparison of course depends significantly on how the chemical shifts are referenced (as well as other parameters).
[48] a) C. Worrell, J. W. Verhoeven, W. N. Speckamp, *Tetrahedron* **1974**, *30*, 3525–3531; b) L. Toom, A. Kutt, I. Kaljurand, I. Leito, H. Ottosson, H. Grennberg, A. Gogoll, *J. Org. Chem.* **2006**, *71*, 7155–7164.
[49] The latter two reagents oxidize diaza-adamantanones; see ref. [5d].
[50] K. Bowden, E. J. Grubbs, *Chem. Soc. Rev.* **1996**, *25*, 171–177.
[51] a) L. M. Stock, *J. Chem. Educ.* **1972**, *49*, 400–404; b) R. D. Topsom, *Prog. Phys. Org. Chem.* **1976**, *12*, 1–20; c) R. Gleiter, M. Kobayashi, J. Kuthan, *Tetrahedron* **1976**, *32*, 2775–2781; d) G. Spanka, P. Rademacher, *J. Org. Chem.* **1986**, *51*, 592–596.

[52] P. Geneste, I. Hugon, C. Reminiac, G. Lamaty, J. P. Roque, *Bull. Soc. Chim. Fr. Part 2* **1976**, 845–846.
[53] a) C. A. Grob, P. W. Schiess, *Angew. Chem.* **1967**, *79*, 1–14; *Angew. Chem. Int. Ed. Engl.* **1967**, *6*, 1–15; b) C. A. Grob, *Angew. Chem.* **1969**, *81*, 543–554; *Angew. Chem. Int. Ed. Engl.* **1969**, *8*, 535–546.
[54] N. Risch, U. Billerbeck, B. Meyerroscher, *Chem. Ber.* **1993**, *126*, 1137–1140.
[55] N. Risch, M. Langhals, T. Hohberg, *Tetrahedron Lett.* **1991**, *32*, 4465–4468.
[56] That the 3,5-substituents are *cis* diequatorial is verified by coupling constants; the α-hydrogen (to the ketone) couples with the β-hydrogen with ^{3}J(H,H) ≈12 Hz.
[57] T. Scherer, W. Hielkema, B. Krijnen, R. M. Hermant, C. Eijckelhoff, F. Kerkhof, A. K. F. Ng, R. Verleg, E. B. Vandertol, A. M. Brouwer, J. W. Verhoeven, *Recl. Trav. Chim. Pays-Bas* **1993**, *112*, 535–548.
[58] *SHELXTL6*, Bruker-AXS, Madison, Wisconsin, USA, **2000**.
[59] P. v. d. Sluis, A. L. Spek, *Acta Crystallogr. Sect. A* **1990**, *46*, 194–201.
[60] A. L. Spek, *J. Appl. Crystallogr.* **2003**, *36*, 7–13.

Received: August 6, 2007
Published online: November 22, 2007

